

# Development of a wind tunnel model for supporting research on aero-servo-elasticity and control of wind turbines

Carlo L. Bottasso, Filippo Campagnolo, Alessandro Croce, Luca Maffenini

*Politecnico di Milano, Milano, Italy, [carlo.bottasso@polimi.it](mailto:carlo.bottasso@polimi.it)*

## 1 INTRODUCTION

Purely aerodynamic models of wind turbines, i.e. models whose scope is the representation of the sole aerodynamic phenomena taking place on a wind turbine, have been developed and tested by, among others, Oku et al, 1996; Hand et al, 2001; Vermeer et al, 2003; Snel et al, 2007; Schepers and Snel, 2007. The design of scaled aerodynamic models of wind turbines is extremely challenging, because of the large scaling factors mapping a multi-MW wind turbine (rotor diameter of the order of 100 m) into the necessarily small wind tunnel model (rotor diameter of the order of a few meters); this in turn implies large differences in the Reynolds number. Nonetheless, it is clear that aerodynamics is only one of the coupled phenomena that take place on a wind turbine and whose understanding is crucial for the most effective design and operation of these machines. In fact, design loads on wind turbines are dictated by transient phenomena, where the effects of structural deformations and of the closed-loop control laws used for regulating the machine play a very major role. Such effects are clearly completely missed by purely aerodynamic models.

In this work we describe the aero-servo-elastic model of a wind turbine, developed at the Department of Aerospace Engineering of the Politecnico di Milano under the support of Vestas Wind Systems A/S. The model represents the 3MW Vestas V90 machine; since the scaled wind turbine has a rotor diameter of 2 meters, it is named V2 in the rest of this document. The model was conceived for conducting experimental investigations on the aero-servo-elasticity of wind turbines in the controlled environment of a wind tunnel, as for example for studying the machine response in extreme operating conditions (e.g., shut down in high winds, operation at high yaw angles, response following failures of on-board sub-systems, etc.), something that is difficult to do in the field. The model can also support research on advanced pitch-torque control laws, on load and wind observers, as well as a variety of other aero-elastic investigations such as the study of the effects of loads induced by wake impingement caused by upstream wind turbines. We believe that such wind tunnel activities could profitably and cost effectively support and complement similar investigations and testing trials conducted in the field. Furthermore, measures conducted on the model can be used for the validation of CFD and aero-servo-elastic codes.

In order to enable such research activities, the scaled wind turbine model was designed under the following requirements:

- The model should be reasonably realistic from the aerodynamic point of view, notwithstanding the unavoidable mismatch in the Reynolds number;
- The model should be aero-elastically scaled, i.e. it should correctly represent the lowest rotor and tower modes and their relative placement with respect to the harmonic excitations;
- The model should be actively controlled by individual blade pitch and torque inputs in real-time, as done on a real wind turbine;
- The model should provide to the control laws at least the same on-board measurements available on modern wind turbines, including blade loads.

In the following pages we describe the scaled wind turbine model developed through this research effort and we report on the results of some testing activities aimed at verifying its characteristics, including a preliminary investigation on the aerodynamic performance.

## 2 MODEL DESIGN

### 2.1 Aero-elastic scaling

The non-dimensional parameters governing the dynamics of wind turbines can be derived in the basis of Buckingham  $\pi$  Theorem (Buckingham, 1904; Barenblatt, 1986) and are represented by the tip-speed-ratio (TSR) ( $\lambda = \Omega R/V$ ), Reynolds ( $Re = \rho Vc/\mu$ ), Froude ( $Fr = V^2/gR$ ), Mach ( $M = V/a$ ) and Lock ( $Lo = C_{L\alpha}\rho cR^4/J$ ) numbers, non-dimensional natural frequencies ( $\tilde{\omega}_i = \omega_i/\Omega$ ), and non-dimensional time ( $\tau = \Omega t$ ), where  $\Omega$  is the rotor angular speed,  $R$  the rotor radius,  $V$  the wind speed,  $\rho$  the air density,  $c$  the blade chord,  $\mu$  the air viscosity,  $g$  the gravitational acceleration,  $a$  the speed of sound,  $C_{L\alpha}$  the slope of the lift curve,  $J$  the flapping inertia of the blade,  $\omega_i$  the  $i$ -th structural natural frequency and  $t$  time. Scaling laws were here derived by the following criteria:

- The exact enforcement between the scaled and full scale models of the same values of TSR (same kinematics), Lock number (same ratio of aerodynamic to inertial forces) and non-dimensional natural frequencies (same Campbell diagram, i.e. same relative placement of harmonic excitations and natural frequencies), which implies

$$\lambda_M = \lambda_P, \quad Lo_M = Lo_P, \quad \tilde{\omega}_{iM} = \tilde{\omega}_{iP}, \quad (1)$$

where  $(\cdot)_M$  indicates quantities of the (scaled) model, and  $(\cdot)_P$  quantities of the physical (full scale) system;

- A best compromise between the Reynolds mismatch  $Re_M/Re_P$ , which is related to the quality of aerodynamics of the scaled model, and the speed-up of scaled time  $t_M/t_P$ , in order to avoid an excessive increase in the control bandwidth; in fact very high control frequencies would make it difficult to test advanced control laws, which is one of the goals of the project, since such laws might possibly imply non-negligible computational loads but still need to be operated in real-time on the model. By letting  $n_i = t_M/t_P$ , then  $Re_M/Re_P = n^2/n_i$ , where  $n = R_M/R_P$  is the length scale factor, which is dictated by the wind tunnel dimensions. The design of best compromise can then be expressed as the following minimization

$$\min_{n_i} (k^2 n^2/n_i + n_i), \quad (2)$$

which yields  $n_i = kn$ , where  $k$  is a weight factor in the cost function. This new definition of the scaling laws does not match the Froude number on the model, which is acceptable unless very large machines are considered, and corresponds to Mach scaling for the choice  $k = 1$ .

The scaling factors of the principal physical quantities resulting from the scaling laws defined above are reported in Table 1.

Table 1. Scaling factors used for mapping the V90 into the V2 characteristics.

Quantity	Scaling factor
Length Ratio $n$	1/45
Time Ratio	1/22.84
Velocity Ratio	1/1.97
Power Ratio	1/15477
Rotor Speed Ratio	22.84
Torque Ratio	1/353574
Reynolds Ratio	1/88.64
Froude Ratio	11.6
Mach Ratio	1/1.97

The resulting rated power of the V2 wind turbine is 193.8 W at a rated rotor speed of 367 rpm. The average Reynolds number, which on the V90 is in the range  $4 \div 5 \cdot 10^6$ , on the scaled model is only in the range  $5 \div 6 \cdot 10^4$ . To account for such large differences, the blade was designed using the special low-Reynolds airfoils AH79-100C (Althaus, 1980) and WM006 (Olesen, 2009), both equipped with transi-

tion strips. The former airfoil was used in the inboard section for  $r/R \in [0.137, 0.423]$ , while the latter in the outboard one for  $r/R \in [0.654, 1]$ . Not to alter the aerodynamic characteristics of the airfoils, interpolations of the cross sectional shapes were limited to a relatively small transition region between the inboard and outboard sections, i.e. for  $r/R \in [0.423, 0.654]$ , and at the root region to smoothly deform the inboard airfoil into the blade root cylinder.

The blade span-wise chord distribution was geometrically scaled from the original one; on the other hand, to account for the change of airfoils between full scale and scaled blades, the blade twist was modified to yield an optimal span-wise distribution of the axial induction factor.

## 2.2 General configuration

The general arrangement of the hub and nacelle systems is shown in Figure 1. The figure shows the model without spinner, nacelle and tower covers and with one single blade, for clarity.

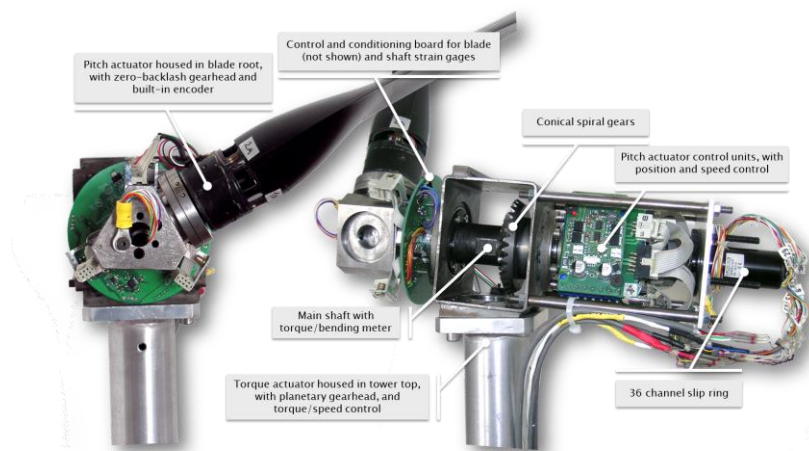


Figure 1. General arrangement of the hub and nacelle systems of the aero-servo-elastic model. The model is shown without nacelle, spinner and tower covers, for clarity, with one single non-aero-elastic carbon-fiber blade with strain-gages.

The blades are mounted on the hub with two bearings, and house in their hollow roots zero-backlash pitch motors with built-in relative encoders. At the blade roots, strain gages provide bending load measurements. The figure shows non-aero-elastic carbon-fiber blades (see later on Section 2.3), that were machined in the cylindrical root region to obtain four small bridges, so as to increase the load-induced strains and improve the accuracy of the strain gages mounted on the same bridges. The shaft was also machined for a similar reason, and hosts strain gages that measure the shaft torsional and bending loads. Two electronic boards, one in front (not shown in the picture) and one behind the hub, provide for the control and conditioning of, respectively, the blade root and shaft strain gages.

The shaft is mounted on two bearings, held by a rectangular carrying box that constitutes the main structural member of the nacelle. Here an optical relative encoder measures the azimuthal position of the shaft, while a tri-axial accelerometer provides for measurements of the acceleration in the nacelle, used for triggering emergency shut-down procedures and optionally for control purposes. A pair of conical spiral gears connects the shaft with a motor that provides for the torque (and optionally speed) control of the rotor. The torque motor is housed in the top of the tower; compressed air is blown in at the tower foot and, travelling along the hollow tower, cools the torque motor, before escaping from a small hole in the back part of the tower top.

Behind the nacelle carrying box, the three electronic control boards of the pitch actuators are mounted on the shaft. A 36-channel slip ring occupies the aft part of the nacelle, held in place by a plate connected to the main carrying box by four rods.

The tower is realized by an inner structural member and an outer non-structural cover. The stiffness of the structural tube was designed so that the first fore-aft and side-side natural frequencies of the na-

celle-tower group of the scaled model match the scaled ones of the full scale system; since the mass of the nacelle is higher than the scaled mass of the real wind turbine, the tower stiffness is higher than the scaled stiffness of the real tower. The non-structural cover is realized with Styrofoam. At the foot of the tower, the model is mounted on a balance that provides measurements of the three force and three moment components at the tower base.

### 2.3 Blade design and manufacturing

The design of the aero-elastically scaled blade was particularly challenging, since the blade has a span of about one meter and a weight of only about 70 grams, yet it should exhibit the correct values of scaled stiffness and mass along its span so as to match the lowest natural frequencies and mode shapes of the real rotor (specifically, the first two blade flap and the first edge modes, and the first rotor collective in-plane mode). Furthermore, in marked contrast to many aero-elastic models, the present one requires a high quality aerodynamic shape, which rules out the use of the classical non-structural disjoint segments connected to a structural carrying member often used in aero-elastic wind tunnel models. These specifications were satisfied by using a machined Rohacell core, which ensures the right shape to the variable chord and twist blade, and two spar caps made of unidirectional carbon fiber. The width and thickness of the spars was optimized along the blade span to achieve the right stiffness, using the numerical procedures described in Bottasso et al, 2010. The blade surface was covered with a polymeric layer that closes the pores of the Rohacell core and ensures a smooth finish.

Rigid blades were also manufactured using carbon fiber, since they are easier and faster to realize than the aero-elastically scaled ones, and were used for the initial testing of the model and the verification of the aerodynamic performance, as described later on in Section 3.

At first, the aero-elastic blade manufacturing technology was verified and demonstrated on a simple specimen, realized with an untwisted uniform cross section with mass and stiffness properties similar to the ones of the model blade in a typical section at around one third of its span (see Figure 2, at top left). The properties of all materials were characterized with specific tests, including the determination of the temperature dependent elastic and shear moduli of the Rohacell core, and the design was verified with a detailed FEM model. The manufactured specimen was characterized in terms of mass (by weighting), stiffness (by static testing), natural frequencies and mode shapes (by dynamic testing), and shape (by measurement with touch probes). The results of this preliminary investigation showed an acceptable matching of the design values of the lowest three natural frequencies (within about 5%), good repeatability, shape and finishing.

The model blades, shown in Figure 2, were then manufactured using the same technological process and experimentally characterized. The blades have not yet been equipped with strain gages, that will be located in the root region on the carbon spar caps.

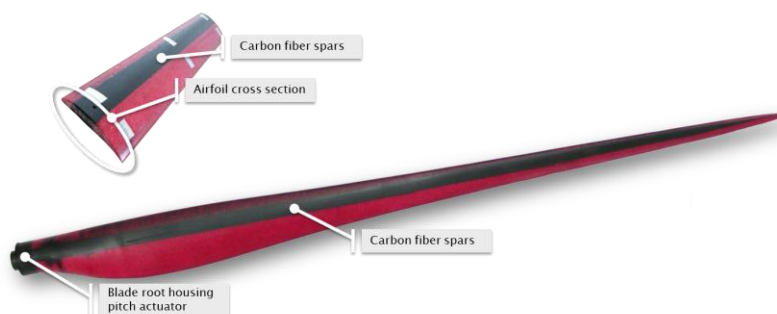


Figure 2. Specimen of uniform properties (at top left) and aero-elastically scaled blade.

In order to have multiple measurement points of the loads along the span, we are working on the integration of Fiber Bragg Grating (FBG) (Hill and Meltz, 1997) sensors in the blade design. At the moment we have realized blade specimens, similar to the ones described previously, placing the optical fi-

bers between two plies of the carbon spar caps. The specimens have been statically tested, with fully satisfactory results in terms of accuracy, linearity and repeatability. Aero-elastically scaled blades with FBG sensors will be manufactured and tested shortly, and we are equipping the model with an electro-optical slip ring that will replace the 36-channel electrical one shown in Figure 1.

#### 2.4 Data acquisition, control and model management system

The architecture of the data acquisition, control and management system is shown in Figure 3.

The experimental model is controlled by a hard-real-time module implementing a supervisor of the machine states and pitch-torque control laws, similarly to what is done on a real wind turbine. Two implementations of this system have been developed, one using a real-time patch of the Linux operating system (<https://www.rtao.org>) running on a standard PC, and the other using the industrial wind turbine Bachmann M1 system (<http://www.bachmann.info>). The control module receives all on-board model sensor readings (including shaft torque/bending-meter, balance strain gages, blade strain gages, rotor RPM and azimuth, blade pitch and nacelle accelerometer), as well as the wind tunnel sensor readings (including wind speed, air temperature and humidity), and sends demands to the pitch and torque motors. The control logic includes the use of a pitch-torque control law, or a simple trimming mode that regulates the machine at given values of RPM and blade pitch setting. The supervisor switches between possible machine states (parked, power production, shut down, run up, etc.), and handles emergencies.

An operator control station implements software for the management of the experiment, and for the data logging, post-processing and visualization of all measurements.

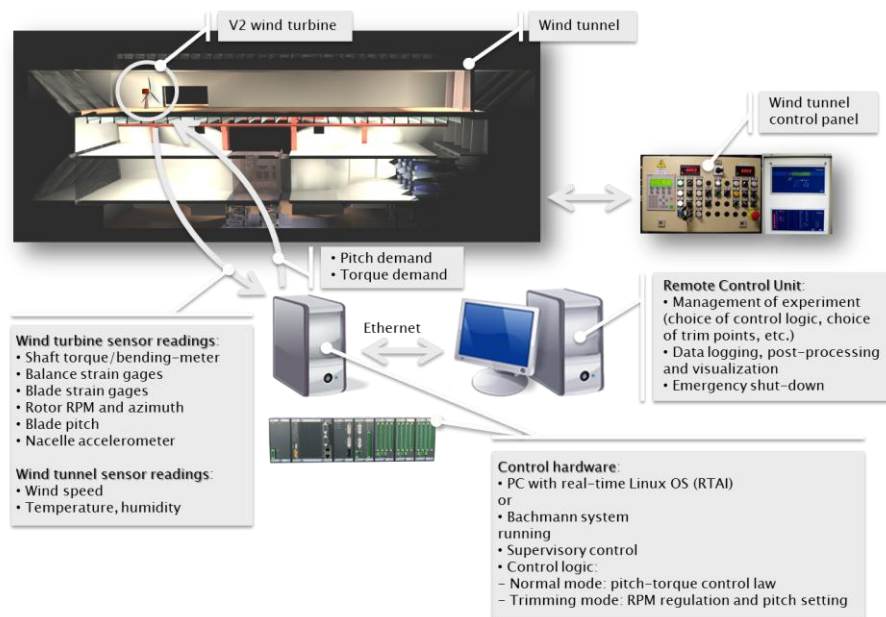


Figure 3. Data acquisition, control and model management system.

#### 2.5 Support equipment

The wind turbine model is complemented by a number of support tools for its testing, calibration and maintenance. A test bench is used for the hardware-in-the-loop verification of the nacelle-rotor system, where the aerodynamic torque on the rotor is provided by a brushless motor on the basis of real-time simulations conducted with a reduced order model. In addition, specific support tools were designed for the calibration of the shaft and blade root strain gages, and for setting the zero of the pitch and azimuth encoders with an accuracy of  $\pm 0.1$  deg. The alignment of the rotor axis with the wind tunnel wind direction is performed by using a small laser emitter, which is placed at the hub center.

## 2.6 Simulation environment

A comprehensive aero-elastic simulation environment has supported all phases of the wind turbine model design, including the determination of loads, of the aero-elastic response of the machine, and the testing of control laws. Mathematical models of the full scale and scaled wind turbines were developed with the code Cp-Lambda (Code for Performance, Loads and Aeroelasticity by Multi-Body Dynamic Analysis) (Bottasso and Croce, 2009-2011), based on a finite-element multibody formulation (see Bauchau et al, 2001 and references therein). The full scale mathematical model was based on data provided by the sponsor, while the mathematical model of the scaled wind turbine was based on its geometric, structural and aerodynamic characteristics, including wind tunnel data of the low-Reynolds airfoils that equip the model blades. Structural cross sectional characteristics of the blade were computed with the composite blade analysis code ANBA (Anisotropic Beam Analysis) (Giavotto et al, 1983), and verified with detailed three-dimensional FEM models when necessary.

The aerodynamic and aero-elastic blade designs were conducted with the wind turbine multi-disciplinary design code Cp-Max (Code for Performance Maximization) (Bottasso et al, 2010). A CFD model of the rotor was developed with the code ROSITA (Rotorcraft Software Italy) (Biava, 2007), using a Reynolds Averaged Navier-Stokes (RANS) formulation on Chimera grids, and used for further verification of the blockage effects due to testing in the relatively small Aeronautical Test Section of the wind tunnel (see later on Sections 2.7 and 3).

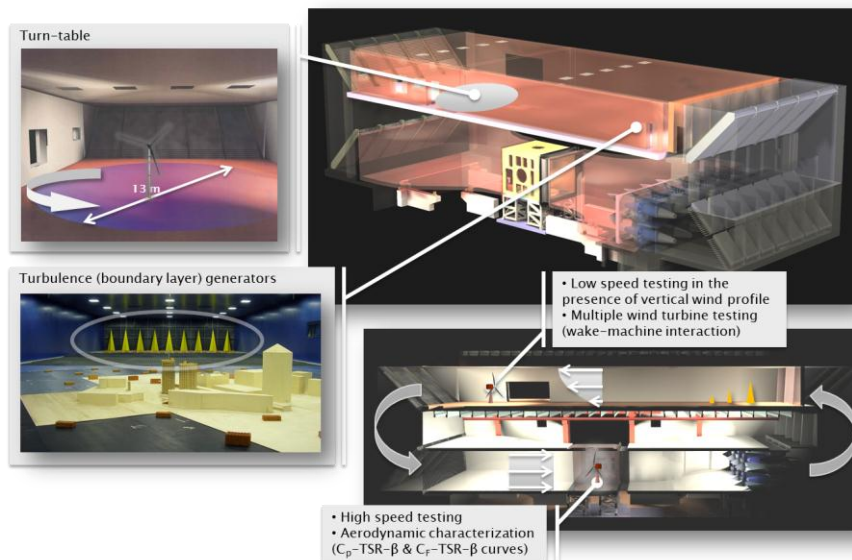


Figure 4. The Wind Tunnel of the Politecnico di Milano.

## 2.7 Wind tunnel

The model operates in the Wind Tunnel of the Politecnico di Milano, Bovisa Campus. The wind tunnel features a closed-circuit configuration, arranged in a vertical layout with two test rooms in the loop (see Figure 4). The upper leg of the loop hosts the Boundary Layer Test Section, which has a size of 14 m by 4 m, a maximum wind speed of 16 m/s, and a turbulence index smaller than 2%. In this 35 m long constant section test room, the atmospheric boundary layer (turbulence index >25%) can be simulated by using active and/or passive turbulence generators, which include spires and fences placed at the test room entrance as well as smaller elements placed on the floor of the test room to increase its roughness. By adjusting the position and size of such devices, one can realize different turbulence scales and vertical wind profiles. The model is mounted on a 13 m diameter turntable, which allows for the changing of the yaw angle of the wind incident over the model rotor.

The Aeronautical Test Section, which is housed in the lower leg of the loop, is 4 m wide, 3.8 m high and 6 m long. Here it is possible to perform tests in a closed test section and in an open jet. The maxi-

mum wind velocity is 55 m/s and the turbulence level is smaller than 0.1%. The test section is equipped with a turntable with a diameter of 2.5 m, and a traversing system located behind the model for wake measurements. Both tests at constant and varying wind speeds (active velocity control) can be performed.

### 3 PRELIMINARY RESULTS

A preliminary investigation on the aerodynamic characteristics of the machine was conducted in the low-turbulence Aeronautical Test Section, with wind speeds from 4 to 9 m/s, rotor speeds from 330 to 400 rpm, TSRs from 5 to 11 and blade pitch settings from -5 deg to 5 deg. The model was equipped with carbon-fiber rigid blades with root strain gages, and two different configurations of transition strips applied on the blade suction side at 5% and 23% chord, with span-wise varying thickness and width.

The rotor aerodynamic performance in terms of power and thrust coefficients as functions of TSR and blade pitch is shown in Figure 5; torque was measured using the shaft torque-meter and thrust by using the tower foot balance, after removing the contribution due to tower drag. The wind tunnel data was corrected for a non-negligible blockage effect ( $\pi R^2/A_{\text{section}} = 0.207$ ) by applying the disk actuator method proposed by Bahaj et al, 2007, and verified by CFD conducting simulations of the experiment with and without wind tunnel walls.

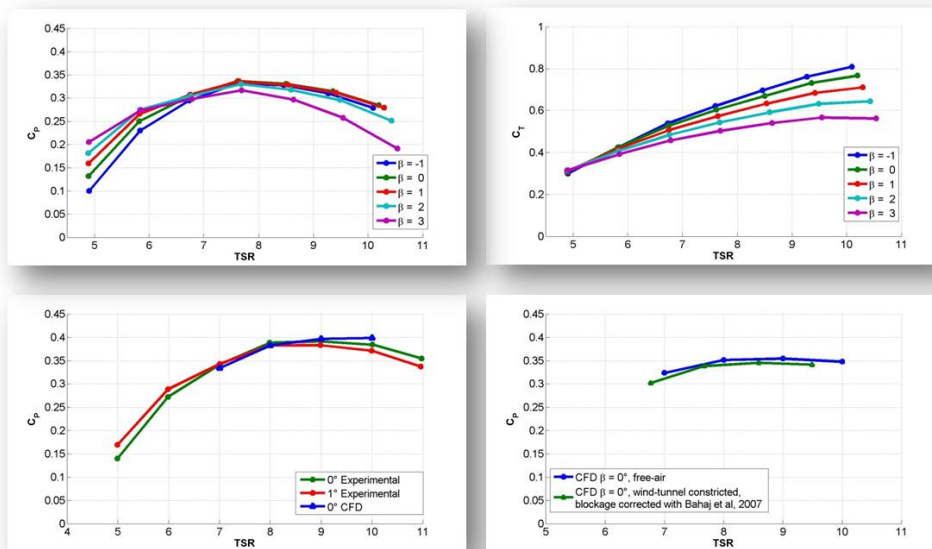


Figure 5. Experimentally measured blockage corrected power (top left) and thrust (top right) coefficients vs. TSR for varying pitch; comparison of experimental and RANS CFD predictions with wind tunnel constriction (bottom left), and validation of blockage correction by CFD predictions in free air (bottom right).

### 4 CONCLUSIONS

The paper has described the design and implementation of what we believe to be the first aero-servo-elastic actively-controlled wind tunnel model of a multi-MW wind turbine. Characterization and initial testing of the machine has shown that the experimental apparatus satisfies the design requirements, in terms of reasonably good aerodynamic characteristics, correct placement of the lowest natural frequencies with respect to the rev harmonics, active control of blade pitch and rotor torque, and on-board data acquisition; furthermore, the design seems reliable and robust, with a good repeatability of all measurements.

Future efforts will continue on multiple fronts. On the model side, work is underway for further improving the aerodynamic characteristics of the blades by modifying the moulds so as to enhance the shape quality of the leading edge, and by optimizing the transition strip dimensions and locations; further work is underway for completing the implementation and integration of FBG sensors on board the aero-elastic blades. Testing work will be developed for demonstrating the capability of conducting maneuvers and the testing of individual blade pitch control laws, as well as for a more complete characterization of the aerodynamics of the machine, including the study of its wake. Such activities are supported by an ongoing effort aimed at the Large Eddy Simulation (LES) modeling of the whole wind tunnel experimental apparatus, including passive turbulence generators, wind tunnel walls and wind turbine model.

## 5 ACKNOWLEDGMENTS

The present project is funded by Vestas Wind Systems A/S, whose support is gratefully acknowledged. The authors wish to thank Bachmann Electronic GmbH for their contribution to the development of the real-time control system. The work on FBG sensors is developed in collaboration with Profs. Y. Nam and I. Paek of Kangwon National University in Korea. The authors acknowledge the contribution in the development of this research project of M. Bassetti, P. Bettini, M. Biava, S. Calovi, S. Cacciola, F. Cadei, G. Campanardi, M. Capponi, G. Galetto, P. Marrone, M. Mauri, S. Rota, G. Sala, A. Zasso of the Politecnico di Milano.

## 6 REFERENCES

- Althaus, D., 1980. *Profilpolaren für den modellflug*. Neckar-Verlag Vs-Villingen, Klosterring.
- Bahaj, A.S., Molland, A.F., Chaplin, J.R., Batten, W.M.J., 2007. Power and thrust measurements of marine current turbines under various hydrodynamic flow conditions in a cavitation tunnel and a towing tank. *Renewable Energy* 32, 407–426.
- Barenblatt, G.I., 1996. *Scaling, self-similarity, and intermediate asymptotics*. Cambridge University Press, Cambridge.
- Bauchau, O.A., Bottasso, C.L., Nikishkov, Y.G., 2001. Modeling rotorcraft dynamics with finite element multibody procedures. *Mathematics and Computer Modeling* 33, 1113-1137.
- Biava, M., 2007. RANS computations of rotor/fuselage interactional aerodynamics. Ph.D. thesis, Dipartimento di Ingegneria Aerospaziale, Politecnico di Milano, Milano, Italy.
- Bottasso, C.L., Croce, A., 2009-2011. *Cp-Lambda – User’s Manual*. Dipartimento di Ingegneria Aerospaziale, Politecnico di Milano, Milano, Italy.
- Bottasso, C.L., Campagnolo, F., Croce, A., 2010. Computational procedures for the multi-disciplinary constrained optimization of wind turbines. Scientific Report DIA-SR 10-02, Dipartimento di Ingegneria Aerospaziale, Politecnico di Milano, Milano, Italy.
- Buckingham, E., 1914. On physically similar systems; illustrations of the use of dimensional equations. *Physical Review*, 4:345-376.
- Giavotto, V., Borri, M., Mantegazza, P., Ghiringhelli, G., 1983. Anisotropic beam theory and applications. *Computers & Structures* 16, 403-413.
- Hand, M.M., Simms, D.A., Fingersh, L.J., Jager, D.W., Cotrell, J.R., Schreck, S., Larwood, S.M., 2001. Unsteady aerodynamics experiment phase VI: Wind tunnel test configurations and available data campaigns. NREL National Renewable Energy Laboratory, Technical Report NREL/TP-500-29955.
- Hill, K.O., Meltz, G., 1997. Fiber Bragg grating technology fundamentals and overview. *Journal of Lightwave Technology* 15, 1263-1276.
- Oku, Y., Kump, K., Bruce, E.N., Cherniack, N.S., Altose, M.D., Whale, J., Papadopoulos, K.H., Anderson, C.G., Helms, C.G., Skyner, D.J., 1996 A study of the near wake structure of a wind turbine comparing measurements from laboratory and full-scale experiments. *Solar Energy* 56(6), 621-633.
- Olesen, N.A., 2009. Personal communication. Vestas Wind Systems A/S, Aarhus, Denmark.
- Schepers, J.G., Snel, H., 2007. Model experiments in controlled conditions - Final report. ECN Wind Energy, Technical Report ECN-E-07-042.
- Snel, H., Schepers, J.G., Montgomerie, B., 2007. The MEXICO project (Model Experiments in Controlled Conditions): The database and first results of data processing and interpretation. *The Science of Making Torque from Wind, Journal of Physics: Conference Series* 75.
- Vermeer, L.J., Sørensen, J.N., Crespo, A., 2003. Wind turbine wake aerodynamics. *Progress in Aerospace Sciences* 39, 467-510.